19th Australasian Tunnelling Conference – Acosta-Martínez, Stewart and Hudson-Smith (Eds.)
© 2025 Australian Tunnelling Society, ISBN 978-0-85825-002-4

Assessment of real-time seismic wave velocity in underground mining using laboratory simulations and optimized fuzzy systems

H. Samadi
School of Mining and Geosciences, Nazarbayev University, Astana, Kazakhstan

F. Suorineni
School of Mining and Geosciences, Nazarbayev University, Astana, Kazakhstan

ABSTRACT: Accurate seismic event source location in underground mines is critical for safety and operational efficiency. Conventional microseismic monitoring systems rely on a single input velocity model, updated periodically, which often results in errors due to ever-changing underground conditions, geological complexity, and evolving mine infrastructure. This study proposes a novel approach using discrete physical models that mimic ever-changing underground mining environments, combined with optimized fuzzy inference systems, to predict real-time input velocities for use in source location algorithms, say SIMPLEX. Laboratory tests involved block samples representing varying ground conditions and the use of acoustic emission techniques (AET) with the SAEU3H system to measure wave velocities. Optimized fuzzy inference systems-learning models, particularly particle swarm optimization-adaptive neuro-fuzzy inference system (PSO-ANFIS), achieved strong performance ($R^2 = 0.97$, NRMSE = 0.001, MAPE = 0.0001). The approach enables more accurate, real-time seismic source location, potentially enhancing the effectiveness of seismic monitoring systems in underground mines.

1 INTRODUCTION

Seismicity in mining involves natural or induced earthquakes, with hazards like rockbursts causing fatalities, losses, and operational challenges (Kebeasy 2017). Predicting rockbursts remains difficult due to settings limitations, though risk zones can be identified (Simser 2019). Microseismic monitoring systems help manage seismic hazards by detecting and locating events, but their accuracy depends on velocity models used. Underground mines feature dynamic rock mass conditions, voids, and varying rock types, making static or layered velocity models inadequate (Trifu and Suorineni 2009). Real-time velocity monitoring is ideal but remains a challenge due to complexity, costs, and constant environmental changes in underground mining.

Real-time seismic wave velocity prediction in mining is vital for improving safety, efficiency, and environmental sustainability (Collins et al. 2014). Research over the past two decades highlights the role of seismic wave velocity in understanding stress conditions, rockburst hazards, and mining-induced seismic events (Trifu and Suorineni 2009, Rebuli 2024). Studies have employed various methods, like passive seismic interferometry (Czarny et al. 2016), in situ measurements (Olivier et al. 2015), numerical modelling (Mukhamedyarova et al. 2023), and ambient noise analysis (Czarny et al. 2019), to track velocity changes and link them to underground stress and structural changes. Findings reveal that velocity drops can indicate stress alterations, and factors like geomechanical properties and ever-changing mining conditions also influence long-term velocity shifts. Advanced models, including empirical and artificial intelligence (AI)-based approaches, have been developed to improve prediction accuracy (Wojtecki et al. 2022). As publications in this area increase, the trend reflects a growing recognition of the need for real-time solutions to predict seismic wave velocity and accurately locate seismic events in underground mines. This study focuses on optimized fuzzy-based learning approaches to meet that need.

AI-based models, particularly machine learning (ML) algorithms, have shown promise in predicting seismic wave velocity in underground mining, offering improved accuracy over traditional methods (Duan et al. 2021, Wojtecki et al. 2022). However, most rely on field data already affected by errors from static velocity models, limiting their precision. Recent research, including laboratory-based studies like that of Maksut et al. (2022), mimicked real mine conditions to better understand seismic wave behavior. Despite positive outcomes, advanced hybrid learning approaches remain underexplored.

This study aims to predict seismic wave velocity in real time, addressing the limitations of constant velocity models that fail to capture dynamic ground changes from mining activities. A unique laboratory-generated dataset of 675 samples with 54 features was created, including varying block sizes, geomechanical properties, voids and backfill features, and geometrical properties. These controlled laboratory settings mimicked the dynamic conditions of real-case underground mining. To enhance prediction accuracy, optimized fuzzy-based learning algorithms were introduced.

2 DATA ACQUISITION; LABORATORY SETUP- DATA GATHERING

This section presents a laboratory-based approach using discrete physical modelling to simulate underground mine conditions and study seismic wave velocity. Discrete physical modelling captures snapshots of mine degradation over time, replicating the effects of continuous mining activities. Because real underground environments are complex and unpredictable, the researchers developed a controlled laboratory setup to mimic these changes safely (Figure 1). The main objective was to predict seismic wave velocity under varying underground conditions using the acoustic emission technique (AET), which resembles microseismic monitoring in mines. Experiments were conducted using granite and synthetic rock (sand-cement) cubes of different sizes (150–450 mm), some with central holes to simulate excavation. Hole diameters (50-150 mm) increased with block size to represent mining progression. These holes were also backfilled with varying cement-sand mixtures (based on ASTM C-109 C standard, ASTM 2013), ranging from 0% to 20% cement, cured for different periods (8 hours to 28 days).

Static cracking agents were used to simulate rock fracturing, and pulse waves were generated from a source sensor, with seven others recording wave arrival times. The positioning of sensors and source, along with known coordinates, enabled analysis of wave propagation through blocks with different internal conditions. The experimental setup included SAEU3H AE data systems and high-frequency AET sensors (SR150M and SRI150) suitable for different block sizes. Concrete blocks were cast using ASTM standards to ensure consistency, and uniaxial compressive strength (UCS) tests were conducted on samples from the same mixtures for quality control. AET provided insights into the influence of material properties, hole size, backfill composition, and curing age on seismic wave velocity, establishing a foundational database for real-time seismic monitoring tools in underground mining.

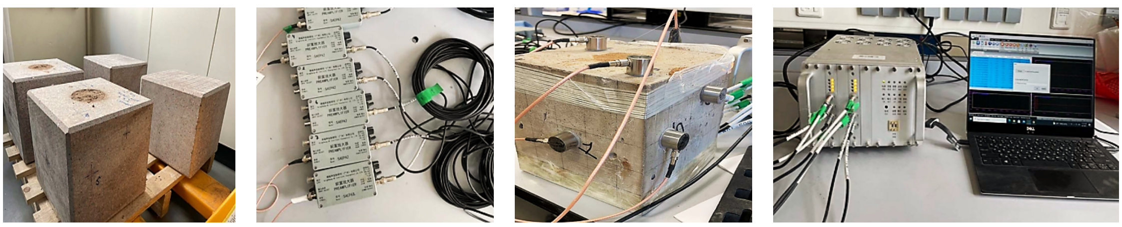

(a) (b) (c) (d)

Figure 1. Acoustic emission (AE) testing setup involved concrete cubes designed to mimic underground mining environments, with specific configurations and sensor placements: (a) block specimens both solid and with drilled holes filled with backfill material, (b) external preamplifier units, (c) AE sensors attached to the cube surfaces, and (d) an AE system connected to a laptop for data collection

3 DATA ANALYSIS; DATA PRE-PROCESSING AND PROCESSING

The laboratory tests provided data from three main sources: 839 readings from the base, 269 from cracked G80 sensors, and 674 from fractured blocks using SR150M sensors. These readings were collected from eight different sensors, with Sensor 1 acting as the pulse source. In total, 1782 data records were collected. Each record included details such as the sensor's location (x, y, z), the distance from the source, wave velocity, arrival time, and the block's physical and geomechanical properties (like size, hole diameter, cement content, curing time, backfill strength, and compressive strength). Only the location of the pulse source was recorded for the source sensor. The blocks, both fractured and unfractured, were evaluated using the rock mass rating (RMR) system (Bieniawski 1989), and wave velocities were measured accordingly.

The data gathered from the laboratory experiments included both numerical and non-numerical types. To make the data easier to analyze and more reliable, it was important to organize and clean it properly. The database was formatted to follow a standard structure and included different geomechanical, physical, and geometric properties. Some data entries had a mix of descriptive and numeric values, and others had missing or duplicated data. To fix this, all data formats were converted into a single float type, and descriptive (qualitative) data was changed into a binary format. After cleaning and organizing the raw data, the final database was created using techniques such as one-hot encoding, handling duplicates, filling missing values, and unifying data types (data handling techniques were completely matched with laboratory investigations). This cleaned database had 675 entries and 54 features. From this, 85% (573 entries) were used for training the models, and 15% (102 entries) were set aside for testing. Full details of this database are listed in Table 1.

Table 1. The summarized features of the laboratory simulation-generated database.

Parameters		Unit	Description
Sample		-	Concrete and granite
Block geometrical properties	Block size (BS)	mm	150, 225, 300, 375, 450
	Hole diameter (HD)	mm	50, 75, 100, 125, 150
Block geomechanical properties	Rock mass rating (RMR)	-	58, 59, 62, 65, 67, 69,70, 71, 72, 74
	Uniaxial compressive strength (UCS)	MPa	9.3, 10.4, 10.5, 11.2, 12.9, 14.04, 15.09, 15.7, 15.8, 17.2, 17.7, 18.5, 19.2, 19.3, 19.7, 20.2, 21.6, 22.3, 22.4, 22.7, 23.01, 23.9, 30.4, 32.1, 34.3, 153
Backfill quality	Cement content (CC)	%	5, 10, 15, 20
	Curing time (CT)	days	8 hours, 1 day, 7 days, 14 days, 28 days
	Backfill strength (BST)	MPa	0.245, 0.353, 0.505, 0.573, 0.651, 0.682, 1.006, 1.07, 1.38, 1.61, 1.99, 2.55, 2.26, 3.102, 4.42, 5.245
Sensor parameters	Location coordinats (X, Y, Z)	-	Min X = 0, Max X = 450 Min Y = 0, Max Y = 450 Min Z = 0, Max Z = 240
	Arrival time (AT)	msec	Min= 0, Max = 4735
	Distance (D)	mm	Min = 82.2, Max = 454
	Velocity (V)	m/s	Min = 0, Max = 4532.6

To prepare the numerical data for analysis, a process called scaling was used. This helps ensure that all data values are on a similar scale, especially when they differ in range or units. In this study, the StandardScaler method was used, which adjusts the data so each feature has a mean of 0 and a standard deviation of 1. This method helps to normalize the data and remove bias in the model. The scaled values included block and backfill details, wave velocity output, and sensor readings such as position, distance, velocity, and arrival times.

4 RESULTS AND DISCUSSION

This part of the paper presents the results from fuzzy-based learning models and explains how different evaluation methods were used to find the most accurate model for predicting seismic wave velocity. Several advanced fuzzy-based supervised learning models, combined with optimization techniques, were used to estimate seismic wave velocity (V_{ave}). These models include particle swarm optimization- Mamdani fuzzy inference system (PSO-MFIS), particle swarm optimization- Takagi Sugeno fuzzy inference system (PSO-TSFIS), and particle swarm optimization- adaptive neuro fuzzy inference system (PSO-ANFIS). Detailed descriptions of these models have been presented in the literature (Sugeno and Takagi 1983, Walia et al. 2015, Verma et al. 2019), so they are not repeated in this study. To train and test these optimized models, 85% of the total data (573 samples) was used for training, while the remaining 15% (102 samples) was used for testing. Figure 2 shows the relationship between the predicted values (from FIS models) and the actual measured values (from laboratory tests), along with their distribution histograms. The accuracy and performance of the models were measured using several error metrics, such as mean absolute deviation (MAD), normalized root mean square error (NRMSE), relative standard error (RSE), root mean squared logarithmic error (RMSLE), mean absolute percentage error (MAPE), relative absolute error (RAE), root relative squared error (RRSE), relative root mean square error (RRMSE), and the coefficient of determination (R^2). The results of these evaluations are listed in Table 2. While all the models performed well, the PSO-ANFIS model outperformed the rest in both training and testing.

Table 2. The results of loss functions and evaluation metrics for analyzing the outcomes of optimized fuzzy-based models in prediction.

Factors	PSO-MFIS	PSO-ANFIS	PSO-TSFIS
MAPE	0.0001	0.0001	0.0001
MAD	1.7752	1.6103	1.6003
RRMSE	0.2514	0.1142	0.1181
NRMSE	0.0026	0.0012	0.0019
RSE	0.0482	0.0015	0.0015
RRSE	0.2195	0.0385	0.0387
R^2	0.9640	0.9720	0.9780
RAE	0.1940	0.0974	0.2731
RMSLE	0.0431	0.0284	0.0389

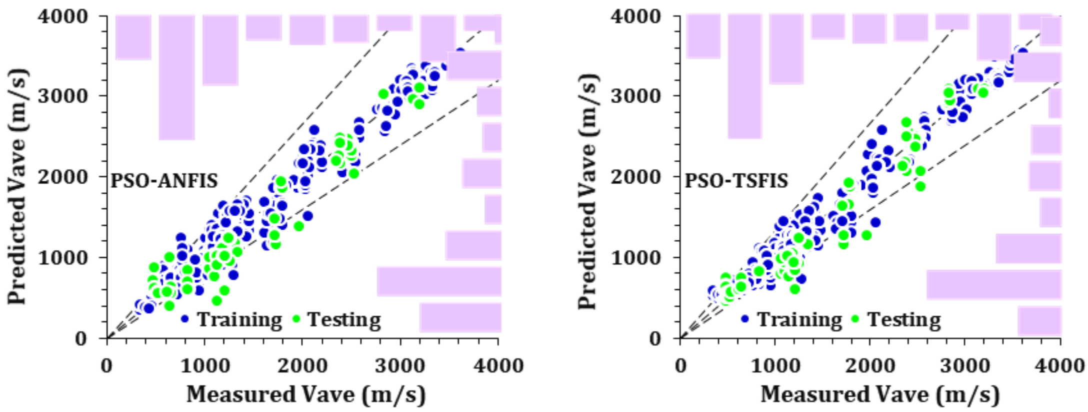

(a) (b)

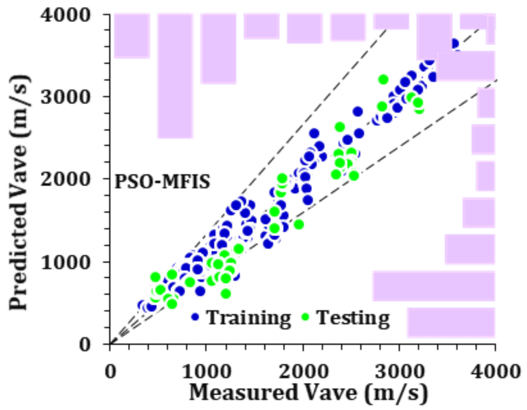

(c)

Figure 2. The correlation between the results of optimized fuzzy-based models and findings from laboratory investigations.

To determine the most accurate model, a score ranking analysis was performed using the results from the different loss functions. Since multiple models and loss functions were used, the total number of scores considered was 27 (matrix 9 by 3). Figure 3 shows the results of the score ranking analysis. As seen from the ranking (from 1 to 3) based on each model's performance on the loss functions, the PSO-ANFIS had the highest overall score of 25, making it the top predictor network in this study. In contrast, the PSO-MFIS model ranked the lowest with a score of 10, showing lower accuracy than the other models.

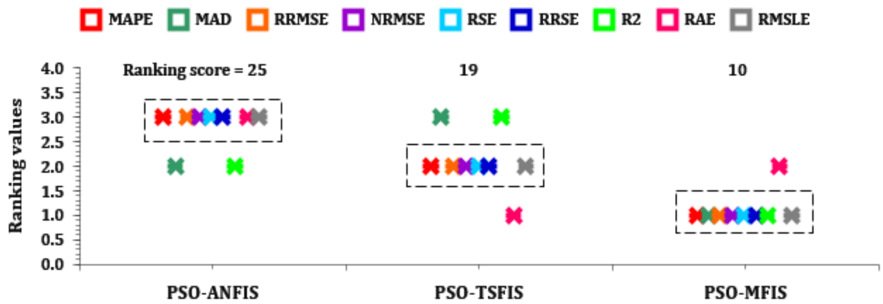

Figure 3. The ranking analysis for optimized fuzzy-based models based on the scores of evaluation metrics.

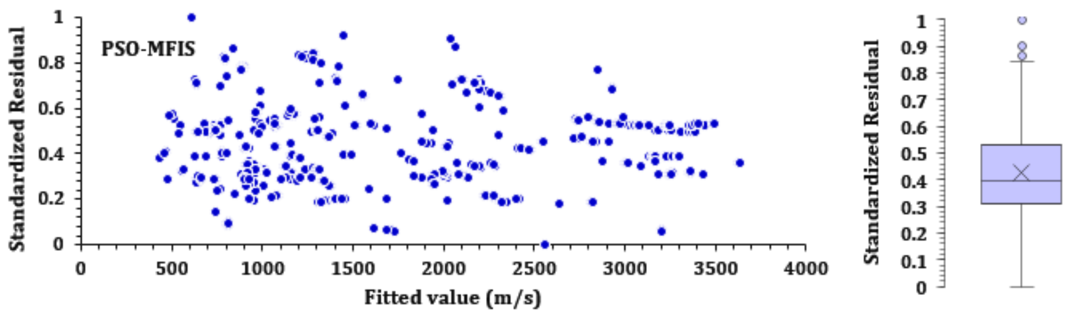

(a)

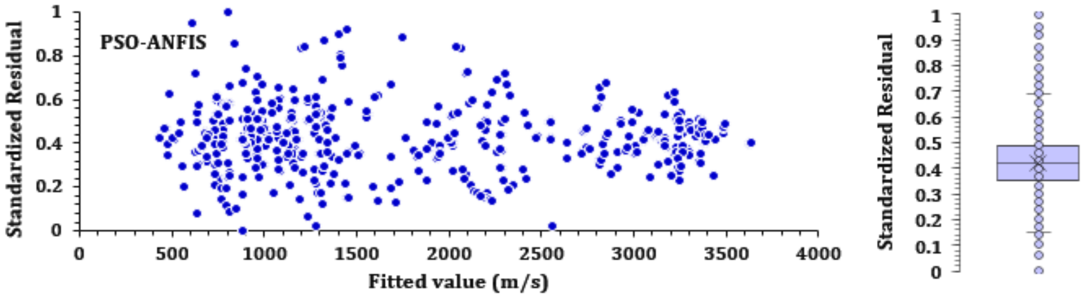

(b)

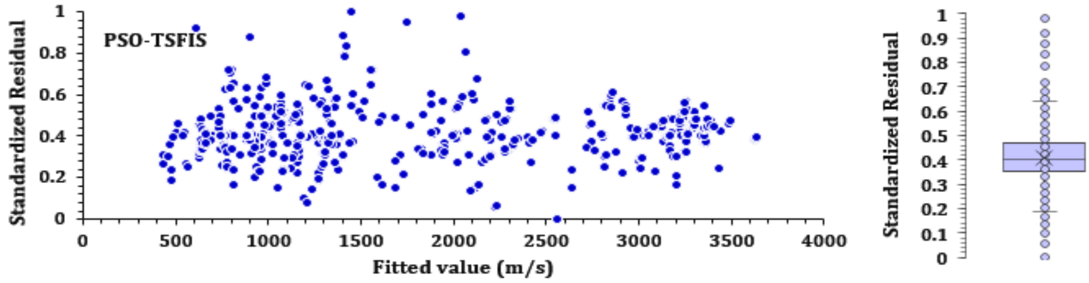

©

Figure 4. The residual plots for each optimized fuzzy-based model.

The residual plot was considered for evaluation to analyze the model behavior. Residual plots for each model are presented in Figure 4, which shows the acceptable behavior of models in prediction with a high accuracy rate. To better understand how each model performed during training and testing, relative error rates were calculated for each sub-dataset, comparing performance across a range of values. The results shown in Figure 5 indicate that all models had error rates within an acceptable range in both phases. This supports the models' accuracy and reliability in predicting V_{ave}, based on their structures, hyperparameters, data distribution, and chosen optimization method, which was PSO.

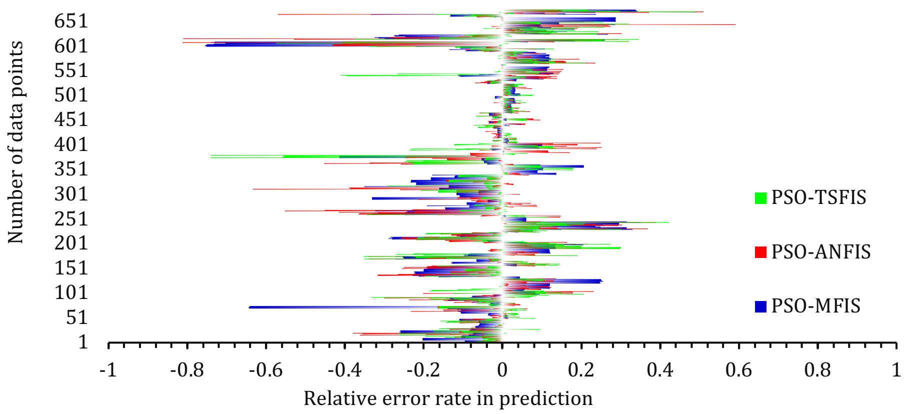

Figure 5. The calculated relative error rate in prediction for each optimized fuzzy-based model.

To compare the performance of models in predicting V_{ave} across different ranges, the predicted and actual values were divided into classes based on the range of V_{ave} values observed. V_{ave} ranged from 335.9 m/s (minimum) to 3206 m/s (maximum) and was divided into seven classes, each with a 500 m/s interval: Class I: 0–500 m/s, Class II: 500–1000 m/s, Class III: 1000–1500 m/s, Class IV: 1500–2000 m/s, Class V: 2000–2500 m/s, Class VI: 2500–3000 m/s, and Class VII: 3000–

3500 m/s. Each class included both measured and predicted values to cover the entire range in the dataset. Based on the laboratory results, the number of data points for each class is: Class I – 30, Class II – 232, Class III – 148, Class IV – 64, Class V – 56, Class VI – 50, and Class VII – 95. A confusion matrix plot (Figure 6) is used to visualize how well each model performed across these classes. The matrix shows that all models were accurate in terms of prediction within each class, with predicted values closely matching the actual ones. This shows that the models had strong prediction performance. The precision rates for each model were: PSO-ANFIS (94%), PSO-TSFIS (90%), and PSO-MFIS (88%).

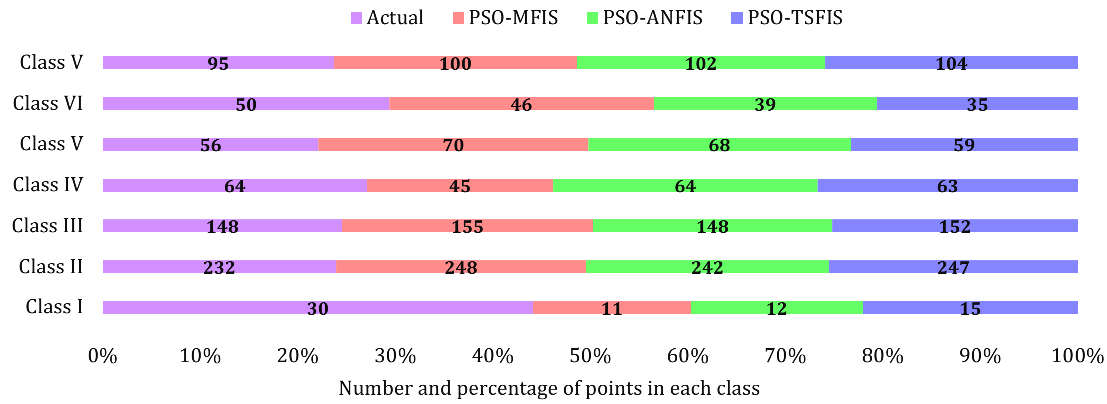

Figure 6. The evaluation of models for each class of V_{ave}- confusion matrix analysis.

To understand how each input factor affects the prediction of the target variable, a sensitivity analysis was done based on optimized fuzzy-based learning models. This analysis shows which inputs have a stronger or weaker effect on predicting V_{ave}. Input factors with higher importance values have more impact on the prediction results, while those with lower values influence the outcome less. Figure 7 presents the results of this sensitivity analysis. The outcomes show that all input factors from the detailed dataset, such as backfill quality, geomechanical features of blocks, block characteristics, location, distance from the source, and arrival time, contribute to predicting V_{ave}. Among them, geomechanical characteristics, backfill quality, and arrival time have a stronger impact. These findings clearly show that using a fixed or constant velocity model is not suitable for locating seismic sources in underground mining, where conditions in the ground change frequently. Instead, a real-time velocity model that adjusts based on current ground conditions is needed to improve the accuracy of seismic event source prediction.

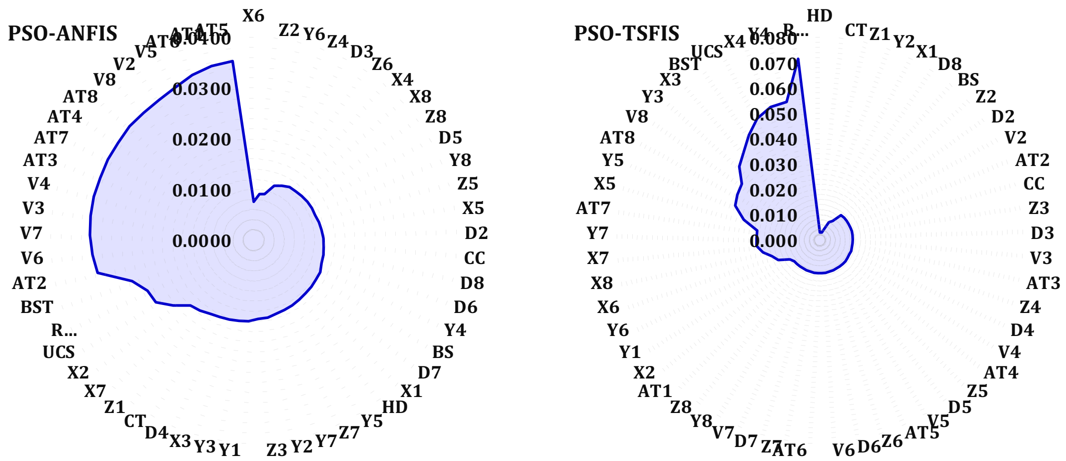

(a) (b)

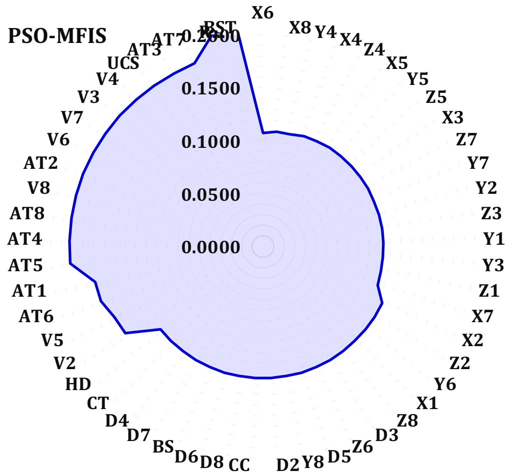

(c)

Figure 7. The sensitivity analysis based on the performance of optimized fuzzy-based models.

5 CONCLUSIONS

This study focuses on predicting seismic wave velocity under constantly changing ground conditions in underground mining, using laboratory-based simulations that mimic real mining environments. Conventional monitoring systems rely on static single-velocity models and numerical simulations, which are often inadequate due to ever-changing conditions in geomechanical properties, geological structures, and void geometries caused by mining activities. To address these limitations, an extensive laboratory dataset, including 675 samples and 54 features, was collected through well-designed laboratory experiments using acoustic emission techniques (AET) and the SAEU3H system, considering the ASTM C-109 C standard to mimic the real case of constantly changing mining conditions. Optimized fuzzy-based models were employed to predict the wave velocity based on the gathered database. The PSO-ANFIS model achieved the best performance with $R^2 = 0.972$, NRMSE = 0.0012, and MAPE = 0.0001. Feature importance analyses showed that geomechanical properties of blocks and backfills, location coordinates, and arrival time significantly influence seismic wave velocity prediction.

ACKNOWLEDGMENT

This work was supported by Nazarbayev University through the Faculty Development Competitive Grant No. 201223FD8835. Additional support was provided by the Nazarbayev University Collaborative Research Programme (CRP) in the data collection stage. The authors acknowledge the contributions of past undergraduate, graduate and post-graduate students, especially: Zarina Mukhamedyarova, Yerkezhan Modenova, and Kimie Suzuki Morales.

6 PREFERENCES

American Society for Testing and Materials (ASTM). 2013. Committee C-1 on Cement. Standard test method for compressive strength of hydraulic cement mortars (Using 2-in or [50-mm] Cube Specimens). ASTM International.

Bieniawski, Z.T. 1989. Engineering rock mass classifications: a complete manual for engineers and geologists in mining, civil, and petroleum engineering. John Wiley & Sons.

Collins, D.S., Pinnock, I., Toya, Y., Shumila, V. and Trifu, C.I. 2014. Seismic event location and source mechanism accounting for complex block geology and voids. In ARMA US Rock Mechanics/Geomechanics Symposium (pp. ARMA-2014). ARMA.

Czarny, R., Pilecki, Z., Nakata, N., Pilecka, E., Krawiec, K., Harba, P. and Barnaś, M. 2019. 3D S-wave velocity imaging of a subsurface disturbed by mining using ambient seismic noise. Engineering Geology, 251, pp.115-127. https://doi.org/10.1016/j.enggeo.2019.01.017

Czarny, R., Marcak, H., Nakata, N., Pilecki, Z. and Isakow, Z. 2016. Monitoring velocity changes caused by underground coal mining using seismic noise. Pure and Applied Geophysics, 173, pp.1907-1916. https://doi.org/10.1007/s00024-015-1234-3

Duan, Y., Shen, Y., Canbulat, I., Luo, X. and Si, G. 2021. Classification of clustered microseismic events in a coal mine using machine learning. Journal of Rock Mechanics and Geotechnical Engineering, 13(6), pp.1256-1273. https://doi.org/10.1016/j.jrmge.2021.09.002

Kebeasy, R.M. 2017. Seismicity. In The geology of Egypt (pp. 51-59). Routledge.

Maksut, Z., Meiramov, R., Yazici, A. and Suorineni, F. 2022. A Machine Learning-Based Microseismic Event Location and Wave Velocity Prediction. In ARMA US Rock Mechanics/Geomechanics Symposium (pp. ARMA-2022). ARMA. https://doi.org/10.56952/ARMA-2022-0166

Mukhamedyarova, Z., Suzuki Morales, K., Suorineni, F. and Madenova, Y. 2023. Numerical modeling of seismic wave propagation in mimicked underground mine models. In ARMA US Rock Mechanics/Geomechanics Symposium (pp. ARMA-2023). ARMA. https://doi.org/10.56952/ARMA-2023-0111

Olivier, G., Brenguier, F., Campillo, M., Roux, P., Shapiro, N.M. and Lynch, R. 2015. Investigation of coseismic and postseismic processes using in situ measurements of seismic velocity variations in an underground mine. Geophysical Research Letters, 42(21), pp.9261-9269. https://doi.org/10.1002/2015GL065975

Rebuli, D. 2024. Seismic response during a mining stoppage. In Deep Mining 2024: Proceedings of the 10th International Conference on Deep and High Stress Mining (pp. 1051-1062). Australian Centre for Geomechanics. https://doi.org/10.36487/ACGrepo/246567

Simser, B.P. 2019. Rockburst management in Canadian hard rock mines. Journal of Rock Mechanics and Geotechnical Engineering, 11(5), pp.1036-1043. https://doi.org/10.1016/j.jrmge.2019.07.005

Sugeno, M. and Takagi, T., 1983. Multi-dimensional fuzzy reasoning. Fuzzy sets and systems, 9(1-3), pp.313-325.

Trifu, C.I. and Suorineni, F.T. 2009, August. Use of microseismic monitoring for rockburst management at Vale Inco mines. In Proceedings of 7th International Symposium on Rockburst and Seismicity in Mines (RASIM7) (pp. 1105-1114).

Verma, N.K., Singh, V., Rajurkar, S. and Aqib, M. 2019. Fuzzy inference network with mamdani fuzzy inference system. In Computational Intelligence: Theories, Applications and Future Directions-Volume I: ICCI-2017 (pp. 375-388). Springer Singapore. https://doi.org/10.1007/978-981-13-1132-1_29

Wang, J.S. and Lee, C.G. 2002. Self-adaptive neuro-fuzzy inference systems for classification applications. IEEE Transactions on Fuzzy systems, 10(6), pp.790-802.

Wojtecki, Ł., Iwaszenko, S., Apel, D.B., Bukowska, M. and Makowka, J. 2022. Use of machine learning algorithms to assess the state of rockburst hazard in underground coal mine openings. Journal of Rock Mechanics and Geotechnical Engineering, 14(3), pp.703-713. https://doi.org/10.1016/j.jrmge.2021.10.011